Journal of Cleaner Production 284 (2021) 124691

Contents lists available at ScienceDirect

Journal of Cleaner Production

journal homepage: www.elsevier.com/locate/jclepro

# Effectiveness and limitation of A-nZVI for restoration of a highly As-contaminated soil

Liang Li [a, b], Xin Wang [a, b, *], Yaoyu Zhou [c], Baoshan Xing [d, **]

[a] College of Resources and Environmental Science, Hunan Normal University, Changsha, 410081, Hunan, China
[b] Key Laboratory of Environmental Heavy-Metal Contamination and Ecological Remediation, Hunan Normal University, Changsha, 410081, Hunan, China
[c] College of Resources and Environment, Hunan Agricultural University, Changsha, 410128, Hunan, China
[d] Stockbridge School of Agriculture, University of Massachusetts, Amherst, MA, 01003, USA

ARTICLE INFO

*Article history:*
Received 23 February 2020
Received in revised form
2 September 2020
Accepted 12 October 2020
Available online 16 October 2020

Handling Editor: M.T. Moreira

*Keywords:*
Arsenic
Air-stabilized nZVI (A-nZVI)
Immobilization
Bioavailability
Biological function

ABSTRACT

To restore highly degraded soil with severe arsenic (As) contamination, effective mitigation of As mobility and bioavailability is considered as the primary step. In this study, the capability of an air-stabilized nano zero-valent iron (A-nZVI) to decrease soil As solubility and leachability was investigated. Further, the effect of A-nZVI on recovery of soil biological function was analyzed by measuring changes in dehydrogenase activity, bacterial community and development of two pioneering plant species. Results showed that A-nZVI exhibited a prominent sorption capacity for both arsenite and arsenate (92.4 and 44.1 mg $g^{-1}$). With A-nZVI application at ≥0.2%, 44.2−74.7% decline in soil As solubility was achieved in neutral water extraction, while consistently higher As extractability was determined with synthetic precipitation leaching procedure (SPLP, pH 4.2). Compared to adjacent forest soil (F-CK), microbial community of the tested soil was featured by 66% lower abundance of *Actinobacteria* while an elevated richness of *Gemmatimonadetes*, both of which showed apparent shift toward F-CK with A-nZVI. 0.2% A-nZVI was most effective in promoting dehydrogenase activity and ryegrass growth. Further, by two-dimensional mapping with the Zr-oxide diffusive gradients in thin films (DGT), averaged DGT-As in rhizosphere of alfalfa (a green manure species) decreased by 47.1% with 0.2% A-nZVI. These results highlight that A-nZVI is critically essential for fixation of soil labile As and thus provides a favorable starting point for recovery of soil health.



## 1. Introduction

Arsenic (As) is class 1 human carcinogen and toxic to most forms of life on earth (Singh et al., 2015). Elevated As accumulation in a wide range of soils has been caused mainly by geochemical processes and anthropogenic activities. In particular, as a result of extensive mining and smelting of metal (loid) ores, a number of degraded lands with high As contamination have been left, which are generally featured by a scarcity of vegetation. As a result of rain erosion, As transport to downstream farmland has been aggravated, leading to a wider range of harm to local population. Take Hunan province in south central China as a typical example. This province is considered as the heartland of Chinese nonferrous mining. It had Asian largest realgar mine (Shimen) and world's largest antimony mine (Xikuangshan) (Sun et al., 2020). Due to historical mining and smelting, a range of highly As-contaminated lands have been deprived of vegetation. In particular, the mountain in close proximity to the former As smelter in Shimen realgar mine has been barren up to date since its closure in 1978 (Fig. 1). It serves as a constant source of As accumulation in downstream farmland soils, leading to much elevated As in local food chain, especially in paddy rice and sweet potato (Yang et al., 2018). This fact and other similar cases suggest the high priority of restoration of degraded soils with high As contamination.

To restore highly contaminated soils, effective reduction of As mobility and bioavailability is considered as the first and most important step. Iron (Fe) (hydr)oxides represent the dominant sink for As sorption in most soils (Wenzel, 2013; Ko et al., 2015; Kumar et al., 2016; Wan et al., 2020), which is mainly attributable to ligand

* Corresponding author. College of Resources and Environmental Sciences, Hunan Normal University, Changsha, 410081, Hunan, China.
** Corresponding author. Stockbridge School of Agriculture, University of Massachusetts, Amherst, MA, 01003, USA.
*E-mail addresses:* wangxin@hunnu.edu.cn, hdhuanjing@163.com (X. Wang), bx@umass.edu (B. Xing).

https://doi.org/10.1016/j.jclepro.2020.124691
0959-6526/

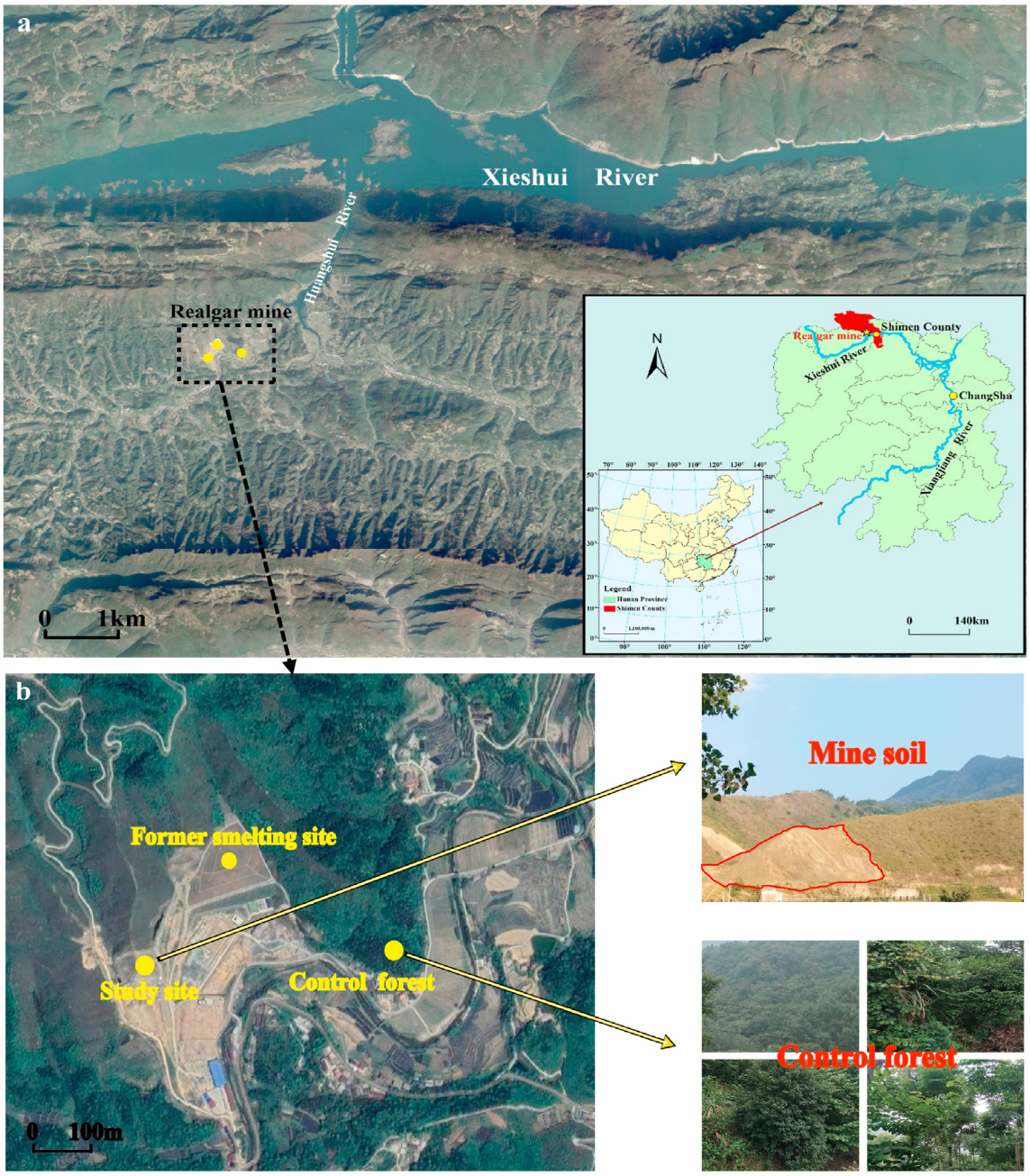


**Fig. 1.** Satellite image (Google Earth Pro) of the tested barren mountain soil and adjecent forest control soil (F-CK) in Shimen realgar mine. Inset shows the location of the field site within Shimen, Hunan, China (a). The barren mountain located at downwind of the former smelter for As trioxide have been almost completely deprived of vegetation. The adjacent forest soil (F-CK) in the upwind direction supported a high diversity of plant species (b).

exchange of As anions for $OH^-$ and $OH_2$ groups, forming inner- and/or outer-sphere complexes (Kumpiene et al., 2008). Compared to Fe (hydr)oxides, zero valent Fe (ZVI) has a prominent advantage of containing up to 3-fold higher Fe by weight. This could be beneficial to soil As immobilization from a long-term perspective (Tiberg et al., 2016). In particular, nano-sized ZVI (nZVI) with much elevated surface area (20–60 $m^2\ g^{-1}$) and unique core-shell structure has exhibited a large capacity of As fixation (Liu et al., 2014; Gil-Díaz et al., 2016; Li et al., 2018; Baragano et al., 2020). Upon application in soils, nZVI particles tend to collide with and adsorb to other compositions and undergo gradual oxidation to Fe (hydr)oxides (Grieger et al., 2010). Therefore, up to date, there is no significant evidence to support that nZVI will bring about apparent environmental risks (Stefaniuk et al., 2016; Phenrat et al., 2019; Li et al., 2020).

Although some previous studies have employed nZVI for *in situ* immobilization of soil As, studies are still lacking in evaluating both the effectiveness and limitation of nZVI in restoration of highly degraded soils. Therefore, in the present work, an air-stabilized nZVI (A-nZVI) was prepared. Arsenic sorption capability was unraveled by sorption kinetics and isotherms test. The underlying mechanisms of As sorption by A-nZVI was investigated using X-ray diffraction (XRD) and X-ray photoelectron spectroscopy (XPS). On this basis, the capability of A-nZVI to reduce soil As solubility and leachability in a highly As-contaminated soil from Shimen Realgar mine was investigated by porewater analysis, chemical extraction

and leaching column test. Further, its effect on recovery of soil biological function was analyzed by measuring changes in dehydrogenase activity, bacterial community and development of two pioneering plant species. Results from this work are expected to provide a better understanding of the potential of nZVI as a useful strategy for restoration of highly As-contaminated soils.

## 2. Materials and methods

### 2.1. Preparation of A-nZVI

The nZVI particles were prepared with aqueous-phase borohydride reduction approach. Briefly, 20 g of $FeSO_4 \cdot 7H_2O$ was dissolved in 1 L of 30/70 (v/v) ethanol/deoxygenated water. Nanoparticles were then synthesized by dropwise addition of 50 mL of 2.88 M $KBH_4$ to $FeSO_4$ solution with vigorous stirring in a three-necked flask under nitrogen. The solution was further stirred for an additional 10 min to achieve full reaction at room temperature. Following complete reduction, nZVI particles were separated from the liquid phase with a magnet and then washed 3 times with ethanol to prevent immediate rusting (Ponder et al., 2000). The washed nZVI particles were spread evenly in a thin layer on an open dish and air-dried (avoid direct sun exposure) at room temperature for 8 h (Ruiz-Torres et al., 2018). The air-dried nZVI particles were designated as A-nZVI and can be kept stable in brown seal bags for at least 10 months. This will largely facilitate its scaled-up transportation compared to traditional nZVI products stored in ethanol.

### 2.2. Characterization of aqueous As sorption with A-nZVI

#### 2.2.1. Sorption kinetics and isotherms test

To identify As sorption kinetics, 250 mg $L^{-1}$ As(III) or As(V) solutions was prepared with A-nZVI being added at a solid/solution ratio of 1:400. No-A-nZVI and no-As control were also included for comparison. The mixtures were shaken at 180 r $min^{-1}$ for a specified period of time from 1 min to a maximum of 24 h at 25 ± 1 °C. At each preset time point, three replicates of the suspension were sacrificed and filtrated through 0.45 μm filters. As concentration in the filtrate was determined by an atomic fluorescence spectrometer (AFS, Haiguang LC-AFS 6500, Beijing). To investigate As sorption isotherms**,** aliquots of 0.1 g of A-nZVI were added into 40 mL of As(III) or As(V) solutions with a set of As concentrations from 1 to 400 mg $L^{-1}$. No-A-nZVI and no-As controls were included. Each treatment had three replicates, all of which were shaken at 180 r $min^{-1}$ for 8 h to reach equilibrium at 25 ± 1 °C. Then the mixtures were filtered (0.45 μm) and As concentrations in the filtrated solutions were measured by AFS.

#### 2.2.2. As sorption mechanisms test

Crystal composition of the surface of both pre- and post-sorption A-nZVI was detected on a computer-controlled X-ray diffractometer (XRD, Bruker AXS, D8 Discover, Karlsruhe, Germany). The valence state and abundance of As, Fe and O on A-nZVI surface was analyzed using X-ray photoelectron spectroscopy (XPS, Thermo fisher-VG Scientific ESCALAB 250Xi, USA). Details are shown in the Supplementary Material.

### 2.3. Soil sampling and experimental setup

The surface soil (0–20 cm) with a total As of 108.5 mg $kg^{-1}$ was collected from a bare mountain in close proximity to a historical As smelter in Shimen realgar mine, Hunan, China (Lat/Long: 29°39′19.4″N, 111°02′34.9″E) (Fig. 1). The soil from an adjacent forest was also collected (F-CK) to provide site-specific remediation target values (Fig. 1). The basic properties of the tested soil and F-CK are shown in Table 1. Details regarding soil analysis are provided in the Supplementary Material.

Aliquots of 0.5 kg of homogenized soil sample were placed into plastic pots (11 cm in diameter × 9.8 cm in height) and amended with 0, 0.2, 0.5, and 1% (w/w) A-nZVI, respectively. Each treatment including F-CK had three replicated pots, which were moistened with deionized (DI) water to approx. 60% of the soil water holding capacity (WHC). The pots were then kept at 22 °C in the dark for 4 weeks with soil moisture being maintained by gravimetric determination every 48 h. At the end of incubation, soil from each pot was divided into three parts: the first part was air-dried and used for chemical analysis, the second was stored at −80 °C for microbial analysis, and the last was used for seedling experiment.

### 2.4. Soil As solubility and leachability analysis

#### 2.4.1. Porewater sampling and analysis

In each pot, one rhizon sampler (MOM-19.21.21F, Rhizosphere Research Products, Netherlands) of 5 cm length was inserted into the soil at ~60% WHC. Porewater samples were extracted by attaching a disposable syringe to each rhizon sampler at 7-d intervals after 24 h equilibration. Porewater As concentrations were determined by AFS.

#### 2.4.2. Single extraction and leaching column test

At the end of 4-week incubation, soil was extracted with DI water to identify A-nZVI effect on soil As solubility under neutral condition (Rodrigues et al., 2010). For comparison, the synthetic precipitation leaching procedure (SPLP, USEPA 1312, 1994a) was employed to investigate the effect of A-nZVI on soil As fixation under acidified condition (Yin et al., 2016). Phosphate extraction was also applied to determine changes in soil As solubility at the presence of P fertilization (García-Salgado et al., 2012).

Following 4-week incubation, leaching column test was carried out with simulated acidic rainwater to investigate the persistence of soil As immobilization by A-nZVI over an extended period of time. According to the actual pH of precipitation in Hunan from 2010 to 2016 (China Meteorological Administration), the leachant pH was adjusted to 4.6 (±0.1) with 4/1 $H_2SO_4/HNO_3$. A total leaching volume of 800 mL was set, which is equivalent to the average rainfall in monsoon season (from April to July) in Hunan. More details regarding the column leaching experiment are provided in the Supplementary Material. The soils from each treatment before and after leaching were air-dried and subjected to As fractionation as suggested by Wenzel et al. (2001) (Table S1).

### 2.5. Soil enzyme activity and bacterial community test

To identify the mitigation effect and any potential harm of A-nZVI, dehydrogenase activity of the incubated soil from each treatment was examined according to Guan (2013).

To characterize A-nZVI-induced changes in composition and diversity of bacterial communities, total soil DNA was extracted from each treatment using a PowerSoil DNA Isolation Kit (MoBio Laboratories, Carlsbad, CA) at the end of 4-week incubation. After purity and quality check on 1% agarose gels, high-throughput sequencing was carried out with the genomic DNA on an Illumina MiSeq PE250 (ALLWEGENE Inc., Beijing, China). The bacterial V4 region of the 16S rRNA genes were amplified using the primer sets 515F-806R (Andrzej et al., 2018). The nucleotide sequences obtained in this work have been deposited in the NCBI GenBank database with the accession numbers from SRR8767402 to SRR8767406. The 16S rRNA gene sequences were assigned to operational taxonomic units (OTUs) by setting a 0.03 distance limit (equivalent to 97% similarity). Based on OTUs, the Chao1 estimator

**Table 1**
Basic properties of the tested barren soil and adjacent forest control soil (F-CK) from Shimen realgar mine (n = 3).

| | pH ($H_2O$) | As (mg $kg^{-1}$) | Fe (g $kg^{-1}$) | Organic matter (%) | Available N (mg $kg^{-1}$) | Available P (mg $kg^{-1}$) | Available K (mg $kg^{-1}$) |
|---|---|---|---|---|---|---|---|
| Tested soil | 7.28 (±0.1) | 108.5 (±1.1) | 26.4 (±0.6) | 1.34 (±0.28) | 41.3 (±0.24) | 10.8 (±0.14) | 129.0 (±0.35) |
| Forest control soil | 5.49 (±0.1) | 75.6 (±1.6) | 34.0 (±0.4) | 2.73 (±0.04) | 98.2 (±1.37) | 60.4 (±0.14) | 196.8 (±1.70) |

for community richness, the Shannon index for community diversity, the metric phylogenetic diversity (PD) whole tree for phylogenetic diversity and Good's coverage for sequencing depth were calculated in QIIME. Relative abundance of major phyla was analyzed. More detailed analysis of the sequencing data are provided in the Supplementary Material.

### 2.6. Seedling experiment

#### 2.6.1. Seed germination test and measurement of ryegrass seedling growth

At the end of four weeks of incubation, soil samples from each treatment were extracted with DI water (1/10, w/v) by shaking overnight. The extraction was used for germination test with ryegrass (*Lolium perenne* L.), which is a typical pioneering species for land reclamation (Qiu et al., 2020). 25 seeds were placed in a Petri dish (diameter 9 cm) with 6 mL of soil extract or DI water (an additional control) in an environmental chamber (28 °C and 60% relative humidity). 2 mL of soil extract or DI water was added every two days and the germination index (GI) was calculated following 7-day incubation. 5 germinated seeds of similar size were then transferred to the soils in different treatments. After 2-month growth, seedling height and root length were measured. Oven-dried biomass was then ground and subject to microwave digestion (CEM MARS 6, Matthews, USA) with $HNO_3$/HCl (EPA Method 3051a) for analysis of As, Fe, K, Ca, Mn, Cu and Zn.

#### 2.6.2. Chemical mapping of bioavailable As in rhizosphere of alfalfa seedlings

Alfalfa (*Medicago sativa* L.), a green manure species commonly used for soil restoration (Luo et al., 2018), was further employed to identify the mitigation effect of A-nZVI on soil As bioavailability. DGT technique with Zr-oxide gel as the binding layer (Easysensor, Nanjing, China) was deployed for two-dimensional mapping of root-available As in alfalfa rhizosphere in the tested soil with (0.2%) and without A-nZVI as well as F-CK. Details of seedling cultivation, rhizobox design, and DGT deployment are given in the Supplementary Material.

After DGT measurement, seedling height and root length of alfalfa were measured. Oven-dried biomass was then ground and subject to microwave digestion (CEM MARS 6, Matthews, USA) with $HNO_3$/HCl (EPA Method 3051a) for total As analysis.

### 2.7. Quality assurance and quality control

All chemicals used in this work were of analytical and guaranteed grade. All plastic and glassware were soaked in 10% (v/v) $HNO_3$ for 24 h and then washed at least three times by DI water prior to use. Containers used in analysis of microbial and enzyme activity were autoclaved. All the treatments including F-CK were performed in triplicate. For the determination of soil As and Fe concentrations, a certified soil reference material (GBW07404, *i.e.*, GSS-4, Chinese National Standard Material Center) and an appropriate number of blanks and calibration standards were included in the digestion and analytical procedures.

All calibration curves for element concentration analysis had an $R^2$ ≥0.999 (AFS for As, AAS for Fe, K, Ca, Mn, Cu and Zn, and UV−Visible spectrophotometer for enzyme activity). At least one calibration standard was run every 20 samples with the detected value being within ±10% of its known concentration. The detection limit is 0.01 μg $L^{-1}$ for AFS and 1.5 μg $L^{-1}$ for flame AAS (FAAS).

### 2.8. Statistical analysis

All the results presented in this study were expressed as means of at least three replicates ± standard deviation and plotted with Origin 2018 and AI (Adobe Illustrator CS6). Differences among the treatments were analyzed by one-way analysis of variance (ANOVA) in SPSS (IBM Statistics 25.0).

## 3. Results and discussion

### 3.1. Efficient As sorption by A-nZVI

The kinetics of both As(III) and As(V) sorption by A-nZVI were shown in Fig. 2a. With initial As(III) or As(V) at 250 mg $L^{-1}$, 79.0% and 32.3% of the ultimate adsorption occurred rapidly within the first 0.5 h. The equilibrium was nearly reached after 2.5 h, with As(III) and As(V) removal rate peaking at 80.6% and 37.8%, respectively. With the extension of adsorption time to 24 h, additional enhancement in the ratio of aqueous As removal was not significant. The better fitting of pseudo-first-order model for As(III) sorption on A-nZVI (Fig. 2a&Table S2) indicates that the sorption rate is not limited by the number of active sites on surface of A-nZVI but only proportional to the real-time As(III) concentration. With regard to As(V) sorption, a better fitting was obtained with pseudo-second-order model (Fig. 2a&Table S2). This could suggest stronger chemical complex of A-nZVI toward As(V), which is the predominant As species in aerobic soils, most likely through specific sorption by forming inner-sphere complexes (Kanel et al., 2006).

It is notable that almost 100% sorption of As(III) and As(V) by A-nZVI can be achieved within 2.5 h at initial As of up to 50 mg $L^{-1}$ (Fig. 2b&S1) which is more than 2 orders of magnitude higher than porewater As concentrations commonly encountered in contaminated oxic soils (up to several hundred μg As $L^{-1}$) (Wenzel et al., 2002; Clemente et al., 2008). This result indicates clearly a high sorption capability of A-nZVI for inorganic As in soil solutions, most likely by forming inner- and outer-sphere surface complexes on the oxide shell of A-nZVI as well as intraparticle diffusion (Kanel et al., 2006; Morin et al., 2008; Yan et al., 2012). Fittings of the Langmuir isotherm equation matched the experimental data well with $R^2$ of 0.99 (Fig. 2b&Table S2), suggesting a monolayer of inorganic As adsorption onto the homogeneous surface of A-nZVI with no interactions between the adsorbed As oxyanions. Moreover, the maximum adsorption of As(III) and As(V) on A-nZVI was predicted to be 92.4 and 44.1 mg $g^{-1}$ (Fig. 2b&Table S2), which were 1.3−308 times higher than those of a range of typical adsorbents for inorganic As exemplified by engineered biochar, clay minerals, and nano-to micro-scaled metal oxides (Table S3). Specifically, a distinctly higher capacity and removal efficiency of A-nZVI toward As(III) than As(V) is in contrast to the often observed stronger scavenging of soluble As(V) by Fe (hydr)oxides relative to As(III) (Singh et al., 2015). This could result partially from the diffusion and enrichment of metallic As ($As^0$) following As(III) reduction into $Fe^0$

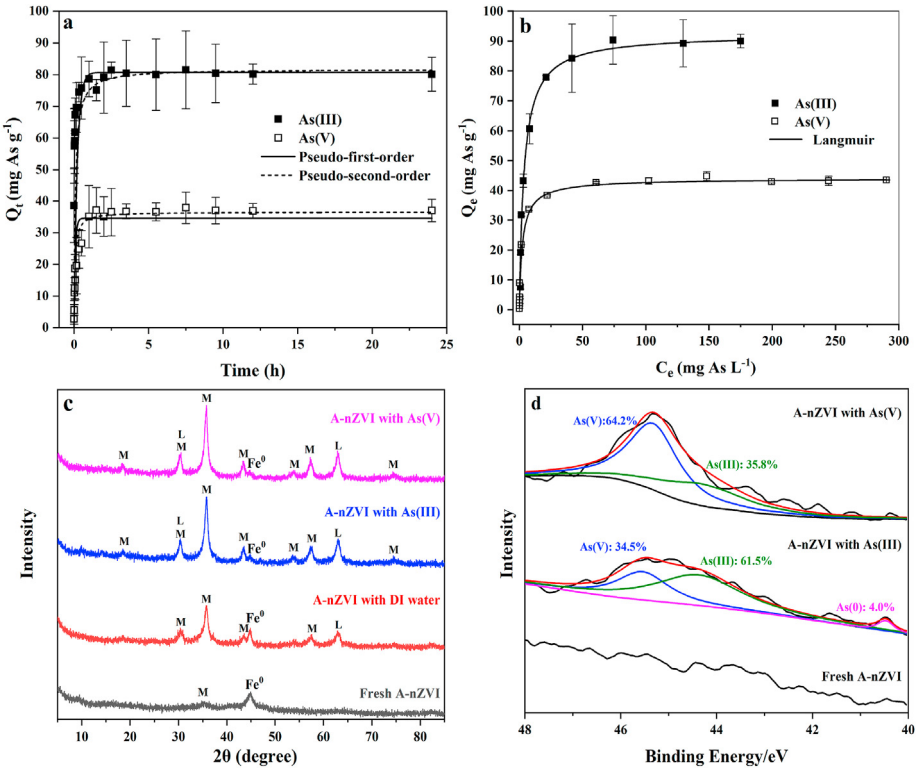


**Fig. 2.** As(III) and As(V) sorption kinetics (a) and isotherms (b) by A-nZVI (T = 25 °C). The initial As(III) and As(V) concentration employed in the kinetic and isotherm study was 250 mg $L^{-1}$ and 1–400 mg $L^{-1}$, respectively. X-ray diffraction analysis (c) and As 3d spectra obtained with XPS spectroscopy (d) of fresh and post-sorption A-nZVI. For XRD and XPS analysis, ratio of A-nZVI to solution = 5 g $L^{-1}$, initial As(III) or As(V) concentration = 100 mg $L^{-1}$, sorption time = 24 h, ambient temperature = 25 ± 1 °C. The XRD peaks have been identified as magnetite/maghemite ($Fe_3O_4$/γ-$Fe_2O_3$) (M), lepidocrocite (γ-FeOOH) (L), and $Fe^0$.

core, as indicated by the presence of an Fe—As intermetallic phase at $Fe^0$ surface based on X-ray absorption analysis (Yan et al., 2012). This unique character of A-nZVI tends to favor an efficient sequestration of highly mobile As(III) in contaminated soils especially under flooded condition. Further, the sorption capacity of A-nZVI for inorganic As species was up to 26.4—44.1-fold higher than that of freeze-dried nZVI (Kanel et al., 2005, 2006), presumably due to the better development of an oxyhydroxide surface of this air-stabilized nanoparticles (Fig. S2) (Ruiz-Torres et al., 2018). This result provides an important indication that controlled passivation of nZVI surface under protection of ethanol with slow exposure to air is not only cost-effective for scaled-up production but also essential for prominent surface complexation of As oxyanions (Fe—O—As).

To understand As sorption mechanisms, fresh and post-sorption A-nZVI samples were comparatively analyzed. Based on XRD, a mixture of magnetite-maghemite ($Fe_3O_4$/γ-$Fe_2O_3$) and lepidocrocite (γ-FeOOH) were present as corrosion products on A-nZVI surface due to the massive oxidation during the sorption process (Fig. 2c) (Horzum et al., 2013). It is interesting to note that the solutions with oxygenated As species exhibited a higher promoting effect on the formation of Fe (hydr)oxides on A-nZVI surface compared to DI water (Fig. 2c). However, no As-containing crystalline mineral phase was detected in the XRD pattern, indicating the dominant sorption of As on amorphous Fe (hydr)oxides phase (Fig. 2c).

Fig. S2a shows the full-range XPS spectra of fresh and As-loaded A-nZVI, unraveling the dominance of Fe (14.7—20.2%) and O (49.5—51.1%) on A-nZVI surface. When A-nZVI was added to As(V) solution, significant amounts of As(III) (35.8%) were detected on the post-sorption A-nZVI surface according to the high-resolution spectra of As 3d (Fig. 2d). When A-nZVI was exposed to As(III) solution, 34.5% and 4.0% of the total surface-bound As was present as(V) and As (0), respectively, with 61.5% remaining as(III) (Fig. 2d). These results support a dual redox function of A-nZVI, which relates closely to its unique core-shell structure (Ramos et al., 2009) containing an outer layer of Fe (hydr)oxides composed mainly of magnetite-maghemite ($Fe_3O_4$/γ-$Fe_2O_3$) and lepidocrocite (γ-FeOOH) and a highly reducing $Fe^0$ core.

The Fe $2p_{3/2}$ spectrum confirmed the co-presence of Fe(II) and Fe(III) on the surface of post-sorption A-nZVI but no $Fe^0$ was detected, confirming the formation of an outer shell of Fe (hydr) oxides (Fig. S2b). Further, oxide oxygen (M-O) in post-sorption A-nZVI increased from 27.5% to 44.4% with a simultaneous decline of $OH^-$ by 24.0% (Fig. S2c), suggesting the newly formed surface complex of Fe—O—As via ligand exchange. In parallel, water adsorbed on the surface of post-sorption A-nZVI also decreased (Fig. S2c), most likely resulting from the competitive adsorption between $H_2O$ and As oxyanion/molecular.

### 3.2. Effect of A-nZVI on soil As mobility

#### 3.2.1. Reduction in soil As solubility by A-nZVI

With 0.2% A-nZVI, a prominent decline (51.4%) in soil porewater As occurred and further increase in A-nZVI rate to 0.5% and 1% led to additional 8.0—24.9% decrease in soil soluble As (Fig. 3a). Similar results were obtained with water-extractable As (Fig. 3b) which represents soil As fraction of the most important environmental concern with regard to its high mobility into surface runoff and groundwater (Rodrigues et al., 2010). These results coincided well with the large As sorption capacity of A-nZVI and highlight the effectiveness of A-nZVI in reducing soil As mobility. Being the most

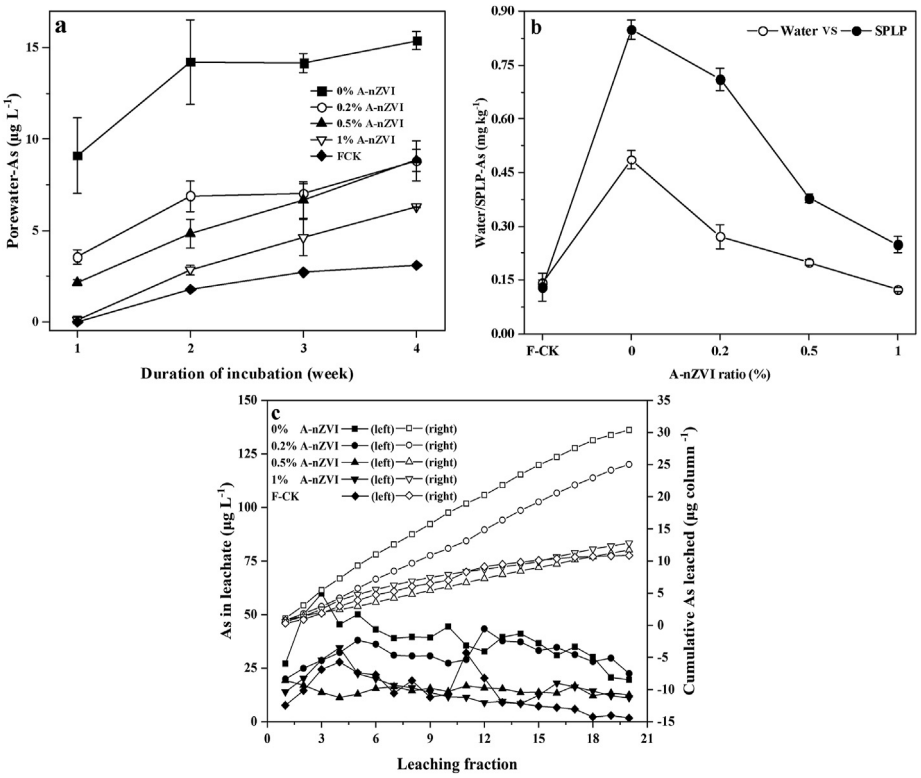


**Fig. 3.** Changes in porewater-As over soil incubation with A-nZVI (a), $H_2O$- and SPLP-extractable As (b), As concentration and cumulative As leached with simulated acid rain (pH = 4.6) (c) at the end of four-week incubation of the tested soil with A-nZVI.

prominent analog of As(V) in terms of p*K*a and thermochemical radius, $KH_2PO_4$-extractable As in A-nZVI-amended soils also exhibited a dose-dependent decrease (9.8–22.6%) (Fig. S3), implying that little risk in enhancing soil As solubility would be posed by P fertilization at the presence of A-nZVI. On the other hand, it reminds of a potential reduction in soil bioavailable pool of some mineral nutrients due to the large capacity of nZVI for sequestration of multiple cations and oxyanions (Li and Zhang, 2007; Li et al., 2018).

In SPLP extraction simulating short-term but intensive acidic precipitation, consistently higher soluble As was obtained as compared to neutral water extraction regardless of A-nZVI amendment (Fig. 3b). For example, only 16.3% decline in SPLP-As was determined with 0.2% A-nZVI, compared to 44.2% in water extraction (Fig. 3b). This difference suggests that As fixation by A-nZVI in the tested soil tends to be impaired by continuous hydrogen input over an extended period of time. It could relate closely to the poor buffering capacity of this degraded soil with significantly lower organic matter (OM) than F-CK (1.3% vs 2.7%) (Table 1), which likely yields a low cation exchange capacity (CEC) of soil and thus elevated Fe dissolution by protonation with less As retention in soil solid phase (Kim et al., 2012; Beesley et al., 2014). Therefore, increasing soil CEC is essential to maintain a longer-term immobilizing effect of A-nZVI toward soil As by counteracting soil acidification.

### 3.2.2. Reduction in soil As leachability by A-nZVI

Leaching column with simulated acid rain was further performed to investigate the persistence of A-nZVI for soil As fixation. With A-nZVI amendment (0.2–1%), 13.0–58.6% decrease in leachate As concentration was determined with 17.6–61.4% decrease in cumulative As leached (Fig. 3c). In particular, with A-nZVI ≥0.5%, soil As leachability exhibited the most prominent decrease to a stable level comparable to that of F-CK. These results demonstrate that A-nZVI is effective for *in situ* fixation of As in the tested soil for at least one summer monsoon season, which is primarily attributed to As sorption onto the passivating oxide layer of A-nZVI (Fig. 2&Table S2) and continuous supply of active sorption sites by on-going corrosion (Yan et al., 2012). Further, it is important to note that oxidation of $Fe^0$ is expected to have little acidifying effect to soil, which is considered as a prominent advantage of A-nZVI over Fe salts (Kumpiene et al., 2008).

Consistent with the above results, non-specifically sorbed As in A-nZVI treated soils, which represents the most labile As fraction, exhibited ≥37.8% decline regardless of acid leaching (Fig. S4). As expected, the amorphous Fe (hydr)oxides were the major sink for As sorption in all the tested soils. With A-nZVI amendment, 16.4–69.8% enhancement in As bound to amorphous Fe (hydr)oxides was determined (Fig. S4). However, it should be noted that solubility of prevalent Fe (hydr)oxides in soils (amorphous $Fe(OH)_3$, maghemite, lepidocrocite, hematite, goethite) are sensitive to pH (Schwertmann, 1991), with $Fe^{3+}$ activity increasing 1000-fold for each unit decrease in soil pH (Lindsay, 1980). Therefore, enhancement in acid buffering capacity of the tested soil with CEC-rich ameliorator could help to inhibit Fe dissolution and thus maintain a longer-term effectiveness of A-nZVI in areas subject to acidic precipitation.

### 3.3. Effect of A-nZVI on soil dehydrogenase activity and bacterial community

Dehydrogenase is a sensitive indicator of trace element contamination in soils and has been widely used for evaluation of soil toxicological status (Lyubun et al., 2013; Tan et al., 2017). In this

study, water-extractable As was up to 3.4 times higher in the unamended barren soil than in F-CK, which resulted in an 81.7% lower activity of dehydrogenase in the tested soil relative to F-CK (Figs. 3b & Fig. 4). With A-nZVI application, dehydrogenase activity was enhanced apparently by 28.3–54.9% with simultaneously decreased As solubility (Fig. 4). The significant negative correlation between dehydrogenase activity and water-extractable As ($R = -0.690$, $p < 0.05$) demonstrates the effectiveness of A-nZVI in promotion of soil enzyme activity by depleting bioavailable pool of As. In support of this conclusion, the activities of soil enzymes as exemplified by β-glucosidase, urease, dehydrogenase, acid-phosphatase, alkaline-phosphatase, arylsulfatase, catalase and aminopeptidase exhibited significantly negative correlations with water soluble As in a range of As-contaminated soils, with up to 50% inhibition of enzyme activity being determined at elevated As lability (Bhattacharyya et al., 2008; Abad-Valle et al., 2015; Su et al., 2017). Further, the above result also indicates little toxicity of A-nZVI itself to local soil microbes, which is consistent with findings reported by Fajardo et al. (2019) and Li et al. (2020). Therefore, A-nZVI application can serve an efficient pathway attenuating soil As toxicity, which is a critical prerequisite for ecological rehabilitation of degraded sites in mining areas.

In addition, the positive effect of A-nZVI on recovery of soil biological function following As fixation was also confirmed by the change of diversity and community structure of soil bacterial community. In this work, the diversity of soil bacterial community was analyzed based on high-throughput sequencing of total 16S rRNA from A-nZVI treated soil (Table S5). The values of Good's coverage of all libraries were above 97%, indicating that most diversity had already been captured although new phylotypes would be expected with additional sequencing. The Shannon diversity index differed significantly among the A-nZVI treatments ($p < 0.05$), which peaked in 0.2% A-nZVI group and decreased gradually with elevated incorporation of A-nZVI. Similar to the Shannon index, Chao 1 showed the same trend, with the highest richness of OTUs occurring with 0.2% A-nZVI. The same holds true for the metric phylogenetic diversity (PD) whole tree. These results consistently indicate that 0.2% A-nZVI is most effective for recovery of richness and diversity of bacterial community, providing an essential starting dose of A-nZVI for field-scale application. As shown in Fig. 5, cluster analysis of UPGMA method based on Bray-Curtis dissimilarity revealed that soil bacterial communities from F-CK and the barren soil formed separate clusters. *Proteobacteria, Acidobacteria, Gemmatimonadetes*, *Actinobacteria* and *Chloroflexi* were the five dominant phyla in the tested soil regardless of treatment. Being the most abundant phylum in the tested soil, *Proteobacteria* showed little change in its relative abundance with A-nZVI amendment, implying its high adaptation and tolerance to As contamination (Das et al., 2013). The relative abundance of *Acidobacteria* exhibited 8.0–24.8% decline with A-nZVI amendment, which could be partially related to the increased soil pH by oxidation of $Fe^0$ (Table S6) (Jones et al., 2009). By contrast, the relative abundance of *Actinobacteria* increased proportionally with A-nZVI rate from 7.2% to 44.9%. As suggested by Sheik et al. (2012), *Actinobacteria* generally has a low abundance (~2%) in As-contaminated soils while elevated richness (~46%) in clean soils. Therefore, the significant increase in *Actinobacteria* richness indicates much reduced toxic effect of As by A-nZVI amendment. Similar results were also reported by Frick et al. (2019), who found that recovery of the soil bacterial community was achieved with ZVI amendment which reduced water-extractable As by 27% (Table S4). Moreover, microbial community of the tested soil was featured by 66% lower abundance of *Actinobacteria* while an elevated richness of *Gemmatimonadetes* compared to F-CK, both of which then showed a gradual shift toward that of F-CK with A-nZVI amendment, confirming the beneficial role of A-nZVI in promoting recovery of soil microbial communities.

Taken together, *in situ* fixation of soil As with A-nZVI favors a significant recovery of soil dehydrogenase activity and bacterial community.

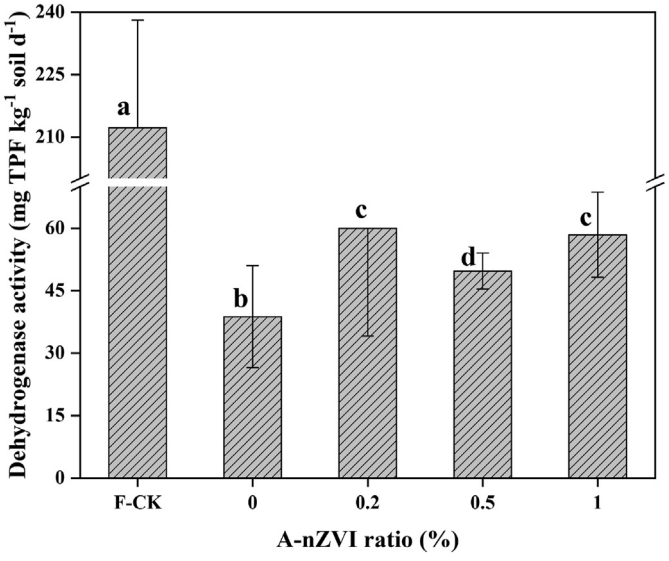


**Fig. 4.** Dehydrogenase activity in F-CK and A-nZVI-amended soils at the end of four-week period of incubation. Bars with the same letter are not significantly different ($p < 0.05$).

### 3.4. Effect of A-nZVI on establishment of pioneering plants

Ryegrass is a typical pioneering species suitable for soil phytostabilization due to its high As tolerance (Karczewska et al., 2017). To evaluate the effect of A-nZVI on ryegrass establishment in the tested soil, Zucconi phytotoxicity test was employed based on the germination index (GI) of seeds (Gil-Díaz et al., 2014; Baragano et al., 2020). According to the germination index (GI) of ryegrass, the tested soil (GI = 49.7%) exhibited high phytotoxicity (Gil-Díaz et al., 2014), indicating that As in this degraded soil had a remarkable inhibitory effect on seed germination of ryegrass. With A-nZVI amendment, attenuated soil phytotoxicity was determined with reduced As bioavailability (Fig. 6a). Consistent with our results are the findings that nZVI amendment at 1–10% showed a promoting effect on germination, plant height and biomass of barley in As-contaminated soil with 5000–7000 mg As kg$^{-1}$ (Table S4) (Gil-Díaz et al., 2014, 2016). In particular, the soil with 0.2% A-nZVI showed no phytotoxicity to ryegrass according to GI value, resulting in comparable seedling height and root length of ryegrass to those in F-CK (Fig. 6a&b). This result was in good agreement with those obtained from dehydrogenase activity and bacterial community test, supporting 0.2% A-nZVI is most effective for recovery of soil biological function.

To further identify the decrease in soil As bioavailability by A-nZVI, 2D mapping of DGT-As in plant rhizosphere was carried out with alfalfa, which is a green manure species and beneficial to soil fertility (Gao et al., 2016). Previous studies have confirmed that DGT-As was closely related to plant available As in As-contaminated soil (Ngo et al., 2016; Qasim et al., 2016; Huang et al., 2019). With 0.2% A-nZVI, an average of 47.1% decline in DGT-As encompassing the rooting zone of alfalfa was determined (Fig. 6c), which was linked to a 32.5% decrease in As concentration in alfalfa seedlings compared to those grown in the unamended soil (Table S7).

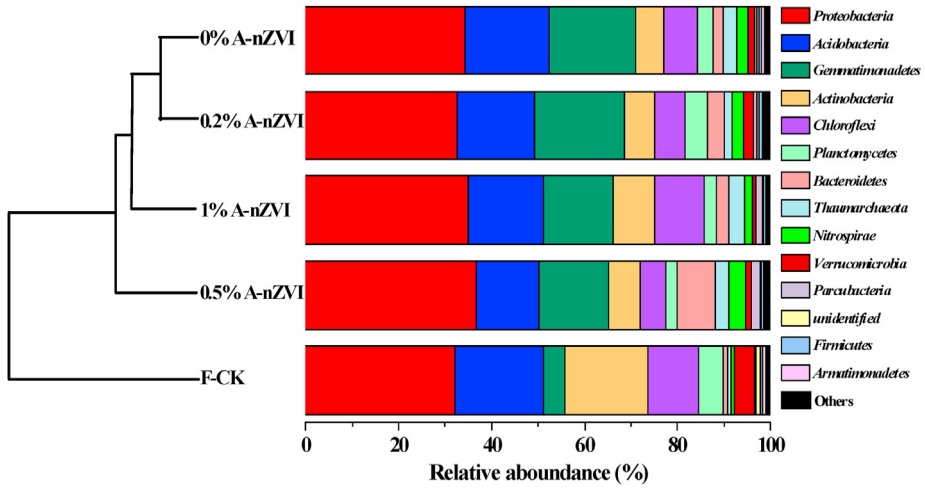


**Fig. 5.** Relative abundance of microbial phyla with H-cluster analysis in F-CK and A-nZVI-amended soils at the end of four-week period of incubation. "Others" included *RsaHf231, GAL15*, *Chlamydiae*, *Tenericutes*, *BRC1*, *SR1_Absconditabacteria*, *TM6_Dependentiae*, *Fusobacteria*, *Elusimicrobia*, *Cyanobacteria*, *Tectomicrobia*, *Saccharibacteria*, *SBR1093*, *Euryarchaeota*, *Hydrogenedentes*, *Chlorobi*, *Peregrinibacteria*, *WS2*, *Microgenomates*, *Candidatus Berkelbacteria*, *Omnitrophica*, *Fibrobacteres* and *FBP*.

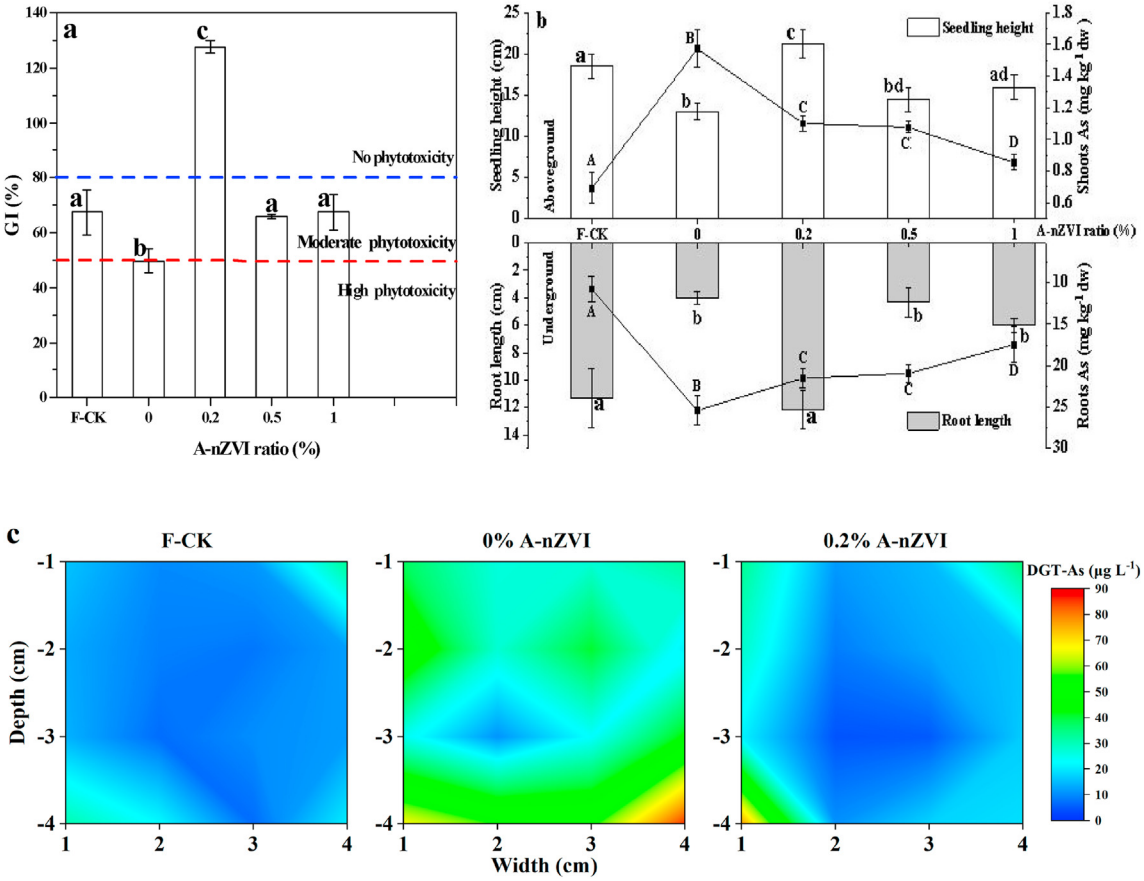


**Fig. 6.** Germination index (GI) (%) of ryegrass after 7-day germination in water extract of F-CK and A-nZVI-amended soils (a). Seedling height, root length and As concentration in ryegrass grown for 2 months in different treatments (b). Two-dimensional profile of DGT-As in the rhizosphere soil of alfalfa after 1-month growth in different treatments (c). The indication of GI for phytotoxicity was derived from Gil-Díaz et al. (2014). Bars with the same letter are not significantly different ($p < 0.05$).

In spite of promoted seedling growth and reduced As bioavailability, As concentration in both ryegrass and alfalfa was still 1.4–2.0 times higher in the A-nZVI treatments than in F-CK (Fig. 6b&Table S7). This detail implies that minimum bioavailability of soil As has not been reached. Efficient As immobilization with A-nZVI can provide a favorable starting point for plant inhabitation in the initial stage of soil restoration. Further attenuation of soil As bioavailability is expected throughout the following community succession.

Another aspect to note is that little risk in soluble Fe toxicity to plants could be posed by A-nZVI application, which has been

partially verified by low ryegrass Fe accumulation (Fig. S5f). Similar result was determined by Gil-Díaz et al. (2014) who found little influence of nZVI treatment on Fe concentration in barley shoot. However, A-nZVI treatment tends to decrease accumulation of some mineral nutrients as represented by K and Zn in ryegrass (Fig. S5), mainly through non-selective sorption and complexation of metal cations as well as oxyanions on A-nZVI surface (Li and Zhang, 2007; Li et al., 2018). This property of A-nZVI is advantageous for *in situ* stabilization of multi-metal-contaminated soils. But for better revegetation, supplementary application of slow-release fertilizer with fortified mineral nutrition could be necessary to improve soil fertility.

## 4. Conclusions and environmental implication

This study identifies that A-nZVI is effective in As immobilization in a smelter-impacted barren soil, leading to significantly lowered As solubility and leachability. Efficient As fixation with A-nZVI is critically essential for recovery of soil biological function and improved inhabitation and growth of pioneering plants. In particular, 0.2% A-nZVI was most effective in promoting soil dehydrogenase activity and reducing As bioavailability in rhizosphere of ryegrass and alfalfa. These results highlight that application of A-nZVI in highly As-contaminated soils is a useful pathway accelerating ecological restoration.

The optimum ratio of 0.2% A-nZVI provides a starting point for its field application and may need further adjustment under local condition. For long-term stabilization of soil As with A-nZVI especially in areas subject to acidic precipitation, supplement of CEC-rich materials is recommended as an assisting measure for hydrogen buffering. Besides, the sorption of A-nZVI toward multiple mineral cations makes it necessary to apply slow-release fertilizers with fortified mineral nutrition for improved growth of pioneering plant species.

## CRediT authorship contribution statement

**Liang Li:** Conceptualization, Data curation, Formal analysis, Investigation, Methodology, Software, Validation, Visualization, Writing - original draft, Writing - review & editing. **Xin Wang:** Conceptualization, Data curation, Funding acquisition, Methodology, Project administration, Resources, Supervision, Writing - original draft, Writing - review & editing. **Yaoyu Zhou:** Conceptualization, Resources, Methodology. **Baoshan Xing:** Conceptualization, Methodology, Writing - review & editing.

## Declaration of competing interest

The authors declare that they have no known competing financial interests or personal relationships that could have appeared to influence the work reported in this paper.

## Acknowledgements

This work was supported by National Natural Science Foundation of China (No. 41977108), Natural Science Foundation for Distinguished Young Scholars of Hunan Province, China (No. 2020JJ2023) and Cultivation Program for National Excellent Youth Science Foundation of Hunan Normal University (XP4180201).

## Appendix A. Supplementary data

Supplementary data to this article can be found online at https://doi.org/10.1016/j.jclepro.2020.124691.

## References

Abad-Valle, P., Álvarez-Ayuso, E., Murciego, A., 2015. Evaluation of ferrihydrite as amendment to restore an arsenic-polluted mine soil. Environ. Sci. Pollut. Res. 22, 6778–6788. https://doi.org/10.1007/s11356-014-3868-6.

Andrzej, T., Marion, H., Poole, P.S., 2018. Absolute quantitation of microbiota abundance in environmental samples. Microbiome 6, 110. https://doi.org/10.1186/s40168-018-0491-7.

Baragano, D., Alonso, J., Gallego, J.R., Lobo, M.C., Gil-Díaz, M., 2020. Zero valent iron and goethite nanoparticles as new promising remediation techniques for As-polluted soils. Chemosphere 238, 124624. https://doi.org/10.1016/j.chemosphere.2019.124624.

Beesley, L., Inneh, O.S., Norton, G.J., Moreno-Jimenez, E., Pardo, T., Clemente, R., Dawson, J.J.C., 2014. Assessing the influence of compost and biochar amendments on the mobility and toxicity of metals and arsenic in a naturally contaminated mine soil. Environ. Pollut. 186, 195–202. https://doi.org/10.1016/j.envpol.2013.11.026.

Bhattacharyya, P., Tripathy, S., Kim, K., Kim, S.H., 2008. Arsenic fractions and enzyme activities in arsenic-contaminated soils by groundwater irrigation in West Bengal. Ecotoxicol. Environ. Saf. 71, 149–156. https://doi.org/10.1016/j.ecoenv.2007.08.015.

Clemente, R., Dickinson, N.M., Lepp, N.W., 2008. Mobility of metals and metalloids in a multi-element contaminated soil 20 years after cessation of the pollution source activity. Environ. Pollut. 155, 254–261. https://doi.org/10.1016/j.envpol.2007.11.024.

Das, S., Jean, J.S., Kar, S., Liu, C.C., 2013. Changes in bacterial community structure and abundance in agricultural soils under varying levels of arsenic contamination. Geomicrobiol. J. 30, 635–644.

Fajardo, C., García-Cantalejo, J., Botías, P., Costa, G., Nande, M., Martin, M., 2019. New insights into the impact of nZVI on soil microbial biodiversity and functionality. J. Environ. Sci. Health - Part A Toxic/Hazard. Subst. Environ. Eng. 54, 157–167. https://doi.org/10.1080/10934529.2018.1535159.

Frick, H., Tardif, S., Kandeler, E., Holm, P.E., Brandt, K.K., 2019. Assessment of biochar and zero-valent iron for in-situ remediation of chromated copper arsenate contaminated soil. Sci. Total Environ. 655, 414–422. https://doi.org/10.1016/j.scitotenv.2018.11.193.

Gao, X.Y., Shi, D.Y., Lv, A., Wang, S.Y., Yuan, S.L., Zhou, P., An, Y., 2016. Increase phosphorus availability from the use of alfalfa (*Medicago sativa* L.) green manure in rice (*Oryza sativa* L.) agroecosystem. Sci. Rep. 6, 36981. https://doi.org/10.1038/srep36981.

García-Salgado, S., García-Casillas, D., Quijano-Nieto, M.A., Bonilla-Simón, M.M., 2012. Arsenic and heavy metal uptake and accumulation in native plant species from soils polluted by mining activities. Water Air Soil Pollut. 223, 559–572. https://doi.org/10.1007/s11270-011-0882-x.

Gil-Díaz, M., Alonso, J., Rodríguez-Valdés, E., Pinilla, P., Lobo, M.C., 2014. Reducing the mobility of arsenic in brownfield soil using stabilised zero-valent iron nanoparticles. J. Environ. Sci. Health., Part A 49, 1361–1369. https://doi.org/10.1080/10934529.2014.928248.

Gil-Díaz, M., Diez-Pascual, S., González, A., Alonso, J., Rodríguez-Valdés, E., Gallego, J.R., Lobo, M.C., 2016. A nanoremediation strategy for the recovery of an As-polluted soil. Chemosphere 149, 137–145. https://doi.org/10.1016/j.chemosphere.2016.01.106.

Grieger, K.D., Fjordbøge, A., Hartmann, N.B., Eriksson, E., Bjerg, P.L., Baun, A., 2010. Environmental benefits and risks of zero-valent iron nanoparticles (nZVI): risk mitigation or trade-off? J. Contam. Hydrol. 118, 165–183. https://doi.org/10.1016/j.jconhyd.2010.07.011.

Guan, S.Y., 1987. Soil Enzymology and its Research Methods. Agricultural Press, Beijing in Chinese.

Horzum, N., Demir, M.M., Nairat, M., Shahwan, T., 2013. Chitosan fiber-supported zero-valent iron nanoparticles as a novel sorbent for sequestration of inorganic arsenic. RSC Adv. 3, 7828–7837. https://doi.org/10.1039/c3ra23454a.

Huang, R., Wang, X., Xing, B.S., 2019. Removal of labile arsenic from flooded paddy soils with a novel extractive column loaded with quartz-supported nanoscale zero-valent iron. Environ. Pollut. 255, 113249. https://doi.org/10.1016/j.envpol.2019.113249.

Jones, R.T., Robeson, M.S., Lauber, C.L., Hamady, M., Knight, R., Fierer, N., 2009. A comprehensive survey of soil acidobacterial diversity using pyrosequencing and clone library analyses. ISME J. 3, 442–453. https://doi.org/10.1038/ismej.2008.127.

Kanel, S.R., Grenèche, J.M., Choi, H., 2006. Arsenic(V) removal from groundwater using nano scale zero-valent iron as a colloidal reactive barrier material. Environ. Sci. Technol. 40, 2045–2050. https://doi.org/10.1021/es0520924.

Kanel, S.R., Manning, B., Charlet, L., Choi, H., 2005. Removal of arsenic(III) from groundwater by nanoscale zero-valent iron. Environ. Sci. Technol. 39, 1291–1298. https://doi.org/10.1021/es048991u.

Karczewska, A., Gałka, B., Dradrach, A., Lewińska, K., Mołczan, M., Cuske, M., Gersztyn, L., Litak, K., 2017. Solubility of arsenic and its uptake by ryegrass from polluted soils amended with organic matter. J. Geochem. Explor. 182, 193–200. https://doi.org/10.1016/j.gexplo.2016.11.020.

Kim, K.R., Lee, B.T., Kim, K.W., 2012. Arsenic stabilization in mine tailings using nano-sized magnetite and zero valent iron with the enhancement of mobility by surface coating. J. Geochem. Explor. 113, 124–129. https://doi.org/10.1016/j.gexplo.2011.07.002.

Ko, M.S., Kim, J.Y., Park, H.S., Kim, K.W., 2015. Field assessment of arsenic

immobilization in soil amended with iron rich acid mine drainage sludge. J. Clean. Prod. 108, 1073–1080. https://doi.org/10.1016/j.jclepro.2015.06.076.
Kumar, R., Kumar, R., Mittal, S., Arora, M., Babu, J.N., 2016. Role of soil physico-chemical characteristics on the present state of arsenic and its adsorption in alluvial soils of two agri-intensive region of Bathinda, Punjab, India. J. Soils Sediments 16, 605–620. https://doi.org/10.1007/s11368-015-1262-8.
Kumpiene, J., Lagerkvist, A., Maurice, C., 2008. Stabilization of As, Cr, Cu, Pb and Zn in soil using amendments – a review. Waste Manag. 28, 215–225. https://doi.org/10.1016/j.wasman.2006.12.012.
Li, X.Q., Zhang, W.X., 2007. Sequestration of metal cations with zerovalent iron nanoparticles–A study with high resolution X-ray photoelectron spectroscopy (HR-XPS). J. Phys. Chem. C 111, 6939–6946. https://doi.org/10.1021/jp0702189.
Li, Z., Wang, L., Wu, J., Xu, Y., Wang, F., Tang, X., Xu, J., Ok, Y.S., Meng, J., Liu, X., 2020. Zeolite-supported nanoscale zero-valent iron for immobilization of cadmium, lead, and arsenic in farmland soils: Encapsulation mechanisms and indigenous microbial responses. Environ. Pollut. 260, 114098. https://doi.org/10.1016/j.envpol.2020.114098.
Li, Z.T., Wang, L., Meng, J., Liu, X.M., Xu, J.M., Wang, F., Brookes, P., 2018. Zeolite-supported nanoscale zero-valent iron: new findings on simultaneous adsorption of Cd(II), Pb(II), and As(III) in aqueous solution and soil. J. Hazard Mater. 344, 1–11. https://doi.org/10.1016/j.jhazmat.2017.09.036.
Lindsay, W.L., 1980. Chemical Equilibria in soils. Clay Clay Miner. 28 https://doi.org/10.1346/CCMN.1980.0280411, 319–319.
Liu, J., Liu, A.R., Zhang, W.X., 2014. Review on transformation of oxidized nanoscale zero valent iron in environment media. Environ. Chem. 33, 576–583. https://doi.org/10.7524/j.issn.0254-6108.2014.04.009 (in Chinese).
Luo, C.G., Deng, Y.W., Inubushi, K., Liang, J., Zhu, S.P., Wei, Z.Y., Guo, X.B., Luo, X.P., 2018. Sludge biochar amendment and Alfalfa revegetation improve soil physicochemical properties and increase diversity of soil microbes in soils from a rare earth element mining wasteland. Int. J. Environ. Res. Publ. Health 15, 965. https://doi.org/10.3390/ijerph15050965.
Lyubun, Y.V., Pleshakova, E.V., Mkandawire, M., Turkovskay, O.V., 2013. Diverse effects of arsenic on selected enzyme activities in soil-plant-microbe interactions. J. Hazard Mater. 262, 685–690. https://doi.org/10.1016/j.jhazmat.2013.09.045.
Morin, G., Ona-Nguema, G., Wang, Y.L., Menguy, N., Juillot, F., Proux, O., Guyot, F., Calas, G., Brown JR, G.E., 2008. Extended X-ray absorption fine structure analysis of arsenite and arsenate adsorption on maghemite. Environ. Sci. Technol. 42, 2361–2366. https://doi.org/10.1021/es072057s.
Ngo, L.K., Pinch, B.M., Bennett, W.W., Teasdale, P.R., Jolley, D.F., 2016. Assessing the uptake of arsenic and antimony from contaminated soil by radish (*Raphanus sativus*) using DGT and selective extractions. Environ. Pollut. 216, 104–114. https://doi.org/10.1016/j.envpol.2016.05.027.
Phenrat, T., Lowry, G.V., Babakhani, P., 2019. Nanoscale zerovalent iron (NZVI) for environmental decontamination: a brief history of 20 years of research and field-scale application. In: Phenrat, T., Lowry, G. (Eds.), Nanoscale Zerovalent Iron Particles for Environmental Restoration. Springer International Publishing AG, Basel, pp. 1–43. https://doi.org/10.1007/978-3-319-95340-3_1.
Ponder, S.M., Darab, J.G., Mallouk, T.E., 2000. Remediation of Cr(VI) and Pb(II) aqueous solutions using supported nanoscale zero-valent iron. Environ. Sci. Technol. 34, 2564–2569. https://doi.org/10.1021/es9911420.
Qiu, Y., Amirkhani, M., Hilary Mayton, H., Chen, Z., Taylor, A.G., 2020. Biostimulant seed coating treatments to improve cover crop germination and seedling growth. Agronomy 10, 145. https://doi.org/10.3390/agronomy10020154.
Qasim, B., Motelica-Heino, M., Joussein, E., Soubrand, M., Gauthier, A., 2016. Diffusive gradients in thin films, Rhizon soil moisture samplers, and indicator plants to predict the bioavailabilities of potentially toxic elements in contaminated technosols. Environ. Sci. Pollut. Res. 23, 8367–8378. https://doi.org/10.1007/s11356-015-5975-4.
Ramos, M.A.V., Yan, W.L., Li, X.Q., Koel, B.E., Zhang, W.X., 2009. Simultaneous oxidation and reduction of arsenic by zero-valent iron nanoparticles: understanding the significance of the core–shell structure. J. Phys. Chem. C 113, 14591–14594. https://doi.org/10.1021/jp9051837.
Rodrigues, S.M., Henriques, B., Coimbra, J., da Silva, E.F., Pereira, M.E., Duarte, A.C., 2010. Water-soluble fraction of mercury, arsenic and other potentially toxic elements in highly contaminated sediments and soils. Chemosphere 78, 1301–1312. https://doi.org/10.1016/j.chemosphere.2010.01.012.
Ruiz-Torres, C.A., Araujo-Martínez, R.F., Martínez-Castañón, G.A., Morales-Sánchez, J.E., Guajardo-Pacheco, J.M., González-Hernández, J., Lee, T.J., Shin, H.S., Hwang, Y., Ruiz, F., 2018. Preparation of air stable nanoscale zero valent iron functionalized by ethylene glycol without inert condition. Chem. Eng. J. 336, 112–122. https://doi.org/10.1016/j.cej.2017.11.047.
Schwertmann, U., 1991. Solubility and dissolution of iron oxides. Plant Soil 130, 1–25. https://doi.org/10.1007/BF00011851.
Sheik, C.S., Mitchell, T.W., Mitchell, T.W., Rizvi, F.Z., Rehman, Y., Faisal, M., Hasnain, S., McInerney, M.J., Krumholz, L.R., 2012. Exposure of soil microbial communities to chromium and arsenic alters their diversity and structure. PloS One 7, e40059. https://doi.org/10.1371/journal.pone.0040059.
Singh, R., Singh, S., Parihar, P., Singh, V.P., Prasad, S.M., 2015. Arsenic contamination, consequences and remediation techniques: a review. Ecotoxicol. Environ. Saf. 112, 247–270. https://doi.org/10.1016/j.ecoenv.2014.10.009.
Stefaniuk, M., Oleszczuk, P., Ok, Y.S., 2016. Review on nano zerovalent iron (nZVI): from synthesis to environmental applications. Chem. Eng. J. 287, 618–632. https://doi.org/10.1016/j.cej.2015.11.046.
Su, S.M., Zeng, X.B., Bai, L.Y., Williams, P.N., Wang, Y.A., Zhang, L.L., Wu, C.X., 2017. Inoculating chlamydospores of, Trichoderma asperellum, SM-12F1 changes arsenic availability and enzyme activity in soils and improves water spinach growth. Chemosphere 175, 497–504. https://doi.org/10.1016/j.chemosphere.2017.02.048.
Sun, X.X., Kong, T.L., Xu, R., Li, B.Q., Sun, W.M., 2020. Comparative characterization of microbial communities that inhabit arsenic-rich and antimony-rich contaminated sites: responses to two different contamination conditions. Environ. Pollut. 260, 114052 https://doi.org/10.1016/j.envpol.2020.114052.
Tan, X.P., Liu, Y.J., Yan, K.H., Wang, Z.Q., Lu, G.N., He, Y.K., He, W.X., 2017. Differences in the response of soil dehydrogenase activity to Cd contamination are determined by the different substrates used for its determination. Chemosphere 169, 324–332. https://doi.org/10.1016/j.chemosphere.2016.11.076.
Tiberg, C., Kumpiene, J., Gustafssonad, J.P., Marsza, A., Perssone, I., Mench, M., Kleja, D.B., 2016. Immobilization of Cu and as in two contaminated soils with zero-valent iron – long-term performance and mechanisms. Appl. Geochem. 67, 114–152. https://doi.org/10.1016/j.apgeochem.2016.02.009.
Wan, X.M., Lei, M., Chen, T.B., 2020. Review on remediation technologies for arsenic contaminated soil. Front. Environ. Sci. Eng. 14, 24. https://doi.org/10.1007/s11783-019-1203-7.
Wenzel, W.W., 2013. Arsenic. In: Alloway, B.J. (Ed.), Heavy Metals in Soils: Trace Metals and Metalloids in Soils and Their Bioavailability. Springer Netherlands, Dordrecht, pp. 241–282. https://doi.org/10.5860/choice.50-3862.
Wenzel, W.W., Brandstetter, A., Wutte, H., Lombi, E., Prohaska, T., Stingeder, G., Adriano, D.C., 2002. Arsenic in field-collected soil solutions and extracts of contaminated soils and its implication to soil standards. J. Plant Nutr. Soil Sci. 165, 221–228. https://doi.org/10.1002/1522-2624(200204)165:2<221::AID-JPLN221>3.0.CO;2-0.
Wenzel, W.W., Kirchbaumer, N., Prohaska, T., Stingeder, G., Lonmbi, E., Adriano, D.C., 2001. Arsenic fractionation in soils using an improved sequential extraction procedure. Anal. Chim. Acta 436, 309–323. https://doi.org/10.1016/S0003-2670(01)00924-2.
Yan, W.L., Vasic, R., Frenkel, A.I., Koel, B.E., 2012. Intraparticle reduction of arsenite (As(III)) by nanoscale zerovalent iron (nZVI) investigated with in situ X-ray absorption spectroscopy. Environ. Sci. Technol. 46, 7018–7026. https://doi.org/10.1021/es2039695.
Yang, F., Xie, S.W., Wei, C.Y., Liu, J.X., Zhang, H.Z., Chen, T., Zhang, J., 2018. Arsenic characteristics in the terrestrial environment in the vicinity of the Shimen realgar mine, China. Sci. Total Environ. 626, 77–86. https://doi.org/10.1016/j.scitotenv.2018.01.079.
Yin, D.X., Wang, X., Chen, C., Peng, B., Tan, C.Y., Li, H.L., 2016. Varying effect of biochar on Cd, Pb and as mobility in a multi-metal contaminated paddy soil. Chemosphere 152, 196–206. https://doi.org/10.1016/j.chemosphere.2016.01.044.